Title: Acidic Horseradish Peroxidase activity abolish genotoxicity of common dyes

Author: Barbara S. Janović Andrew R. Collins Zoran M. Vujčić Miroslava T. Vujčić

PII: S0304-3894(16)30859-7
DOI: http://dx.doi.org/doi:10.1016/j.jhazmat.2016.09.037
Reference: HAZMAT 18043

To appear in: *Journal of Hazardous Materials*

Received date: 17-5-2016
Revised date: 22-8-2016
Accepted date: 16-9-2016

Please cite this article as: Barbara S.Janović, Andrew R.Collins, Zoran M.Vujčić, Miroslava T.Vujčić, Acidic Horseradish Peroxidase activity abolish genotoxicity of common dyes, Journal of Hazardous Materials http://dx.doi.org/10.1016/j.jhazmat.2016.09.037

Acidic Horseradish Peroxidase activity abolish genotoxicity of common dyes

Barbara S. Janović[a*], Andrew R. Collins[b], Zoran M. Vujčić[c] and Miroslava T. Vujčić[a]

[a] Department of Chemistry, Institute of Chemistry, Technology and Metallurgy, Njegoševa 12, P.O. Box 815, 11000 Belgrade, Serbia.

[b] Department of Nutrition, Institute of Basic Medical Sciences, University of Oslo, PB 1046 Blindern, 0316 Oslo, Norway;

[c] Department of Biochemistry, Faculty of Chemistry, University of Belgrade, Studentski trg 12-16, 11000 Belgrade, Serbia

*Correspondence to: Barbara Janović, Institute of Chemistry, Technology and Metallurgy Department of Chemistry, Njegoševa 12, P.O. Box 815, 11000 Belgrade, Serbia, Tel.: +381 63 556 928. E-mail: bjanovic@chem.bg.ac.rs

Graphical abstract

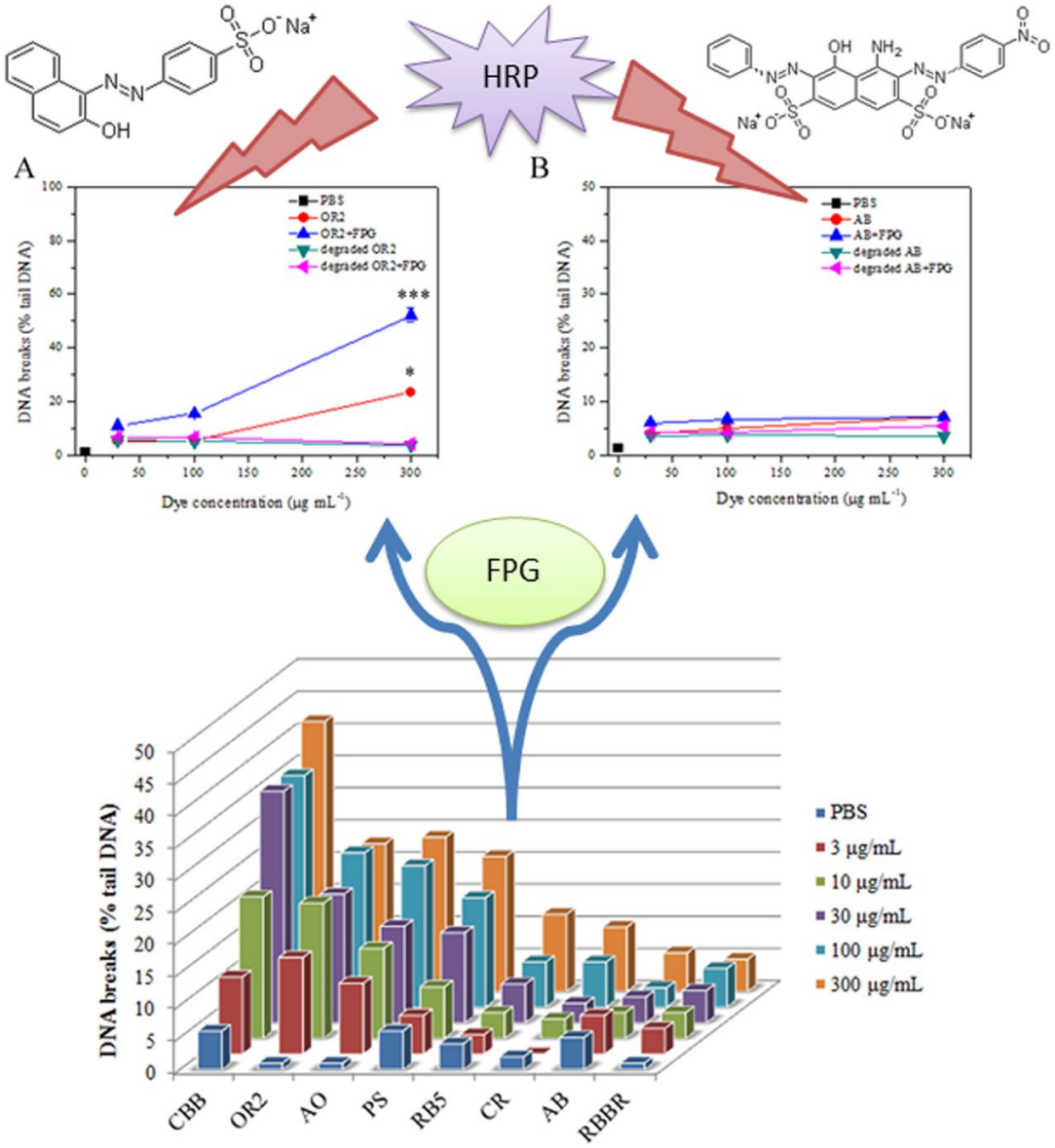

Highlights:

- Decolorization of several types of dye by acidic horseradish peroxidase.
- Evaluation of genotoxicity of eight dyes by medium-throughput comet assay in BEAS-2B cell.
- Detection of DNA damage before and after decolorization using basic and modified comet assay.

- OR2 showed increase in FPG-sensitive sites, while AB showed no increase.
- DNA binding studies were investigated by absorption and fluorescence spectroscopy.

Abstract

The aim of this study was to investigate the impact of dyes on DNA before and after enzymatic decolorization by acidic horseradish peroxidase (HRP-A). The comet assay is easy and feasible method widely used to measure DNA damage and repair. The medium-throughput comet assay was employed for assessment of genotoxic effects of 8 dyes in BEAS-2B cells. We have incorporated a digestion with bacterial endonuclease (formamidopyrimidine DNA glycosylase, FPG) to detect oxidized bases in the case of single and double azo dyes, Orange II (OR2) and Amido Black 10B (AB), respectively. This allowed detection 8-oxo-7,8-dihydroguanine, one of most abundant oxidized bases in nuclear DNA. In the case of AB there was no indication of DNA damage, either strand brakes or FPG-sensitive sites before and after decolorization. The OR2 induced DNA damage (in terms of percentage of DNA in comet tails). Also, the frequency of FPG-sensitive sites increased with OR2 concentration. After decolorization no DNA damaging effects were seen at all. The interaction studies of OR2 and AB, before and after decolorization, with calf thymus DNA has been investigated by absorption and fluorescence spectroscopy. The results provide support for the idea that in some cases enzymatic decolorization contributes to lower genotoxicity potential.

Keywords: DNA damage, comet assay, horseradish peroxidase A, decolorization, dye degradation, DNA interactions.

1. Introduction

Synthetic dyes are widely applied in textile, paper and other industries and discharge of wastewater containing dyes is an ever-growing problem of modern industrial times [1,2]. Since the vast majority of dyes have complex chemical structures, as well as enhanced colored stability, their degradation and removal from wastewaters is a challenging problem [3]. Azo dyes are recalcitrant and resistant to microbial degradation, as well as to other traditional processes [4,5]. Therefore, the need for

new technological solutions for removal of a diversity of dyestuffs from the effluents has led to extensive research in the field of enzymatic approaches to decolorization.

Horseradish peroxidase (HRP) is an oxidoreductase which can catalyze the degradation of numerous aromatic substrates with high efficiency under mild conditions [6]. The majority of dyes in industrial use are azo derivate which makes them potential substrate for HRP [7]. Additional advantage of using isolated enzyme is higher specificity towards individual, potentially dangerous, compounds in the complex wastewaters leading towards better standardization and easy handling. Most significantly there is no dependence on bacterial growth, as in case of microbial decolorization, or generation of huge amount of concentrated sludge or waste, as in physical treatment. HRP is an widely distributed enzyme, isolated from plants, which has showed great stability and activity in broad range of pH and substrate concentration, as well as effective degradation and precipitation of industrially important dyes and phenols [7–9].

Some studies have shown that complex azo dyes can yield aromatic and aryl amines which can be potentially mutagenic and/or carcinogenic [10]. The problem of wastewater treatment cannot be tackled only from the angle of dye and/or xenobiotic removal by oxidative enzyme, in terms of finding the optimal conditions for the degradation process. The biological and genomic impact of dyes, dye metabolites and degradation products must be taken into account. Genotoxic effects can be a result of progressive DNA damage which is partially mediated by reactive oxygen species and has a potential to lead to mutation and development of cancer [11]. Free radicals can be generated by the dye molecule itself, during reductive biotransformation of the azo bond or by products obtained after oxidation [12]. The toxicity of degradation methods and decolorization products must be taken into account. Considering the extensive use of azo dyes, in textile and other industries, the present study aimed to assess the effects of typical synthetic colorants: Orange II (OR2) and Amido Black 10B (AB). The majority of azo-aromatic dyes usually have one or more azo groups (R_1-N=N-R_2), aromatic rings substituted by sulfonate group (-SO3), hydroxyl group (-OH), etc. Among azo dye class, AB is a diazo dye applied for protein staining in biochemical research and in forensic science [13]. Since AB is acid sulfonated dye which reacts with proteins it is used in staining synthetic and natural fibers in garment

and other industries (e.g. paints, inks, plastics) [14]. OR2 is anionic mono azo dye used in several industries such as soaps, wood, hair dyes, textile, cosmetics and leather materials [15]. According to the Scientific Committee on Consumer Safety of EU presented in the SCCS/1382/10 hair dye containing OR2 possess a risk to the health of consumer [16]. Although, OR2 is banned in food industries, some reports indicate their presence in food products in such as tomato sauce, chili and confectionary products[15]. Other report indicate health risk associated with OR2, including the alternation of immunomodulatory effects at non-cytotoxic dose (50 μg ml^{-1}) [17].

Since toxicants can exert different mode of actions deepening upon route of exposure and the organism, in humans, assessments of genotoxic/mutagenic potential should be based upon most similar mammal models [18]. We have applied the comet assay in the measurement of DNA damage effects in horseradish peroxidase decolorization of reactive dye. The comet assay is a sensitive and versatile method for detecting DNA strand breaks within individual cells [19]. The assay was used to investigate how enzymatic decolorization by acidic horseradish peroxidase affects genotoxic potential of dyes. Since exposure to environmental hazardous substance is usually accompanied by DNA oxidation, the modified comet assay, employing FPG, has been used for the first time as for detection of oxidized bases in BEAS-2B cells before and after enzymatic decolorization. This kind of damage to human DNA is the most common one, as it is mainly induced by reactive oxygen species (ROS) after exposure to different environmental agents [20] .The BEAS-2B cells, because of their non-cancerous phenotype, have advantage in the investigation of carcinogenic process such as DNA damage and cell transformation as well as for *in vitro* toxicology testing in the field of pollutants, tobacco products and nanomaterial [21]. In further and more detailed studies, DNA interactions between calf thymus DNA (CT-DNA) and single (OR2) and double azo dye (AB) have been evaluated using several spectroscopic techniques. The binding characteristics of dye and degradation products before and after treatment with HRP-A were analyzed.

2. Materials and methods

2.1. Chemicals

Highly polymerized calf thymus DNA (CT-DNA) was purchased from Serva, Heidelberg. The stock solution of CT-DNA was prepared by dissolving lyophilized CT-DNA in 20 mM Tris-HCl/NaCl buffer pH 7.9 and stored at 4°C in the dark. The concentration of CT-DNA solution was determined by measuring UV absorbance at 260 nm. One optical unit corresponds to 50 μg mL^{-1} of double stranded DNA (based on the known molar absorption coefficient value of 6600 $M^{-1}cm^{-1}$). The ratio of UV absorbance at 260 and 280nm was 1.88 indicating that DNA was sufficiently free from protein.

Horseradish peroxidase (HRP-A) was isolated and purified from the fresh roots of horseradish, harvested near Grabovac (Serbia), as previously described [22]. Peroxidase activity was measured at 25 °C using 0.02 M guaiacol as substrate. The peroxidase assay was done according to the protocol described by Estela da Silva [23]. The absorbance increase in the assay mixture was monitored at 436 nm. One unit of enzyme activity was defined as the amount which catalyzes the conversion of 1 μmol of guaiacol per minute under the assay conditions.

The dyes used in this study are listed in Table 1. All chemicals and reagents were of analytical grade. Dye solutions were prepared as stock solution (2 mg mL^{-1}) in phosphate buffered saline (PBS) from the powdered dyes.

Unless otherwise stated, they were purchased from Merck (Darmstadt, Germany) and Sigma Aldrich (St. Louis, MO, USA). Purified water was obtained from a Milli-Q system (Millipore).

2.2. Decolorization studies

Dyes were diluted in 20 mM bicarbonate buffer pH 9.0 or 20 mM phosphate buffer pH 7.0. Dye solution (300 μg mL^{-1}) was incubated with 20 μL of 3U mL^{-1} HRP-A and 170 μM H_2O_2. Reaction mixtures were incubated 1h room temperature (25 °C) in the dark. Prior to the comet assay, the reaction mixture was treated with catalase (3 U mL^{-1}) in order to remove any excess H_2O_2. The extent of decolorization of the dyes was calculated based on the formula at specific λ_{max}: $D\ (\%) = [(A_i - A_d)/A_i] \times 100$, where A_i is the absorbance of the dye before decolorization and A_d is the absorbance after the decolorization treatment.

The identification of decolorization products after HRP treatment was done according to the protocol described by Zhang [24]. HPLC system (Agilent 1200 Series, Agilent Technologies) equipped with degasser, autosampler, Wakosil II 5C 18RS column (250 mm×4.6 mm i.d., 5 μm particle size) coupled with 6210 time-of-flight LC-MS systems (Agilent Technologies) was used. An isocratic MS compatible method and the mobile phase consisted of 90% methanol and 10% water was used. The flow rate was maintained at 0.2 mL/min. The injection volume was 3 μL for OR2 and 10 μL for degraded OR2 and the column temperature was maintained at 25 °C. A personal computer system running Mass Hunter Workstation software was used for data acquisition and processing. The negatively charged molecular ions were obtained with electrospray ionization (ESI) at atmospheric pressure: the eluted compounds were mixed with nitrogen in the heated nebulizing interface, and polarity was tuned to positive with the following ESI parameters: capillary voltage 3.0 kV, gas temperature 300 °C, drying gas flow rate 8 L/min, nebulizer pressure 40 psig and fragmentor voltage 125 V. Mass spectra were acquired over an m/z (mass-to-charge-ration) range of 50-1000.

2.3. Cell culture

BEAS-2B (human lung epithelial cell line) obtained from ATCC were cultured in Bronchial Epithelial Growth Medium (BEBM®) containing BEGM® kit (Lonza Group Ltd., Belgium). Cells were maintained as monolayer cultures in T25 flasks at 37 °C in a humidified atmosphere with 5% CO_2. Before reaching 80% confluence, cells were washed with PBS and collected using 0.25% trypsin-EDTA (0.53 mM) solution containing 0.5% polyvinylpyrrolidone (Gibco). Cells were placed at 37° C for 2-3 min to facilitate detaching. After the cells were rounded up (detached) under the inverted microscope they were centrifuged (125 x g for 5 min) and resuspended with fresh cultivation medium in new flask. Medium was refreshed every 2–3 days and cells were subcultured every 4–5 days (1500–3000 cells cm^{-2}).

2.4. Treatment of the cells and the comet assay

The medium-throughput format of 12 mini gels per slide was applied. Using the 12-Gel Comet Assay Unit™ (Severn Biotech Ltd) cells in each mini gel were incubated separately with the tested

compounds [25]. The BEAS-2B cells were grown to 80% confluence, washed with PBS, detached by trypsinization and resuspended in fresh medium. Using a Countess™ automated cell counter the concentration of the cells was adjusted, with PBS, to 2.5 x 10^5 cells mL^{-1} and mixed with 4 parts 1% low melting-point agarose (Invitrogen) at 37 °C. Final agarose concentration was 0.8%. Twelve drops (5 μL) of agarose-cell suspension were placed on an agarose-precoated slide using template provided on the metal base of the 12 gel chamber. Five dye concentrations were tested in duplicate with the two control gels on each slide using a format of two rows of 6 mini gels. After embedding, cells in each gel were treated separately with different concentration of dye, before and after the HRP-A treatment, as follows. The slide with 12 gels was placed on the cold metal base, covered with the silicon gasket and clamped in place. Each well in the 12 gel Severn chamber was incubated with 30μl of dye solution at concentrations of 0, 3, 10, 30, 100 or 300 μg mL^{-1}. The same procedure and concentrations were applied for incubation of gels with decolorization products. The chamber was covered with parafilm and incubated on room temperature (25 °C) for 30 min. Before transferring the slides to lysis solution they were washed twice in PBS. Cells were lysed by placing the slides in 2.5 M NaCl, 0.1 M Na_2EDTA, 10 mM Tris with 1% Triton X-100 pH 10 for 1 h at 4° C. The slides were placed in horizontal gel electrophoresis tank in electrophoresis solution (0.3 M NaOH, 0.001 M Na_2EDTA) for 20 min. Electrophoresis was carried out for 30 min at voltage gradient of 1V/cm across the platform at 4° C. Neutralization of the slides was performed by washing them for 10 min in PBS in a staining jar at 4° C. Slides were than fixed by placing them in 70% ethanol for 10 min followed by 10 min incubation in absolute ethanol. Afterwards, slides were allowed to air-dry overnight and were stored at room temperature until further use.

2.5. Enzyme treatment with FPG

For the enzyme incubation with formamidopyrimidine DNA glycosylase (FPG) three identical slides were prepared for incubation with AB and OR2, as well as degradation products. In this case 12 mini gels were treated with 0, 30, 100 and 300 μg mL^{-1} of dye and degradation products. After the lysis gels were washed three times in enzyme buffer (40 mM HEPES pH 8, 0.1 M KCl, 0.5 mM EDTA, 0.2 mg mL^{-1} BSA, pH 8) and slides were transferred to the Severn chamber. To each gel on the slide 30 μL

of buffer or FPG solution was added. The chamber was sealed and placed in thermostat at 37° C for 30 min. Enzyme reaction was stopped by immediately placing the slides in alkaline solution.

2.6. Visualization of comets

DNA was stained by immersing the slides in a staining jar with SYBR Gold (Invitrogen) for 30 min in the dark. Staining solution was prepared according to the manufacturer's instructions in 10 mM Tris, 1 mM EDTA buffer, pH 8. Stained slides were rinsed twice with water and left to dry in the dark. Prior to scoring, a drop of water was put on each gel and the slide was covered with a 24x60 mm coverslip. Scoring of the comets was carried out using semi-automated image analysis system (Comet Assay IV; Perceptive Instruments). On each gel 50 nucleoids were analyzed and the results were expressed as percentage of tail intensity (% of DNA in tail).

2.8. UV-Vis spectroscopy measurements

The UV-visible absorption spectra of dye and dye in the presence of CT-DNA were recorded in the absence and presence of HRP-A and H_2O_2. For UV-visible measurements absorption spectra were recorded using a UV-1800 Shimadzu UV/Visible spectrometer operating from 200 to 800 nm in 1.0 cm quartz cells. The absorbance titrations were performed at fixed dye concentration before and after decolorization while varying CT-DNA (20, 40, 60, 80, 100, 120, 140 and 160 μM final concentration). The reaction mixtures were incubated for 90 min at 37 °C. Afterwards, the UV-Vis absorption spectra were measured against the appropriate buffer as a blank.

2.9. Fluorescence measurements

The competitive displacement assay has been performed by monitoring the changes in the fluorescence spectra of the complex formed between CT-DNA and the fluorescence probe after subsequent addition of the dye or degradation products. The reaction mixture contained fixed concentration of CT-DNA (100 μM) and EB (25 μM) while varying the concentration of dye and degradation products, by successive addition from the stock solutions in 1 mL 40 mM bicarbonate buffer pH 8.4. Reaction mixtures were incubated in the dark at 25 °C for 15 min, before the fluorescence

spectra were obtained. All fluorescence measurements were recorded on a Thermo Scientific Lumina Fluorescence spectrometer (Finland) equipped with a 150W Xenon lamp at room temperature with the slits fixed at 10 nm on excitation and emission beams. All measurements were performed by excitation at 500 nm in the range of 520-700 nm.

The fluorescence quenching data were analyzed according to a modified Stern-Volmer equation, since the dye and degradation products had no obvious fluorescence under the applied experimental conditions [26]. The following equation was applied: $I_0/I=1+Kr$, where I_0 and I represent the fluorescence intensity of the EB-DNA in the absence and presence of dye or degradation products, respectively. *K* is a Stern-Volmer quenching constant, while *r* is the ratio of the concentration of dye or degradation products to that to CT-DNA. *K* was determined by linear regression of a plot of I_0/I against *r*. The double reciprocal plot was obtained using the equation for static quenching: $1/ F_0-F=1/F_0-Kd\ x\ 1/(F_0\ x$ [Q]), where *Kd* is the dissociation constants for the reaction of quenching reagents and fluorophore. *Kd* is defined as the ratio of slope and the intercept obtained from the plot of $1/ (F_0-F)$ vs. $1/$[Q]. Afterward the binding constant was obtained as $K_B=1/Kd$.

2.7. Statistical analysis

All experiments were performed in triplicate. The median %tail DNA for 50 comets was calculated for each of the duplicate gel in the experiments; the mean of the two median values was then calculated. The mean percentage of DNA in the tail is calculated from the independent triplicate experiments using Microsoft Excel software. The final data obtained with the comet assay were analyzed using One-way or Two-ways analysis of variance (ANOVA) followed by the multiple comparison Tukey-Kramer test. The comparisons were carried out against negative control (PBS).

3. Results

3.1. Decolorization by HRP-A

A result of decolorization of dyes by HRP-A is summarized in Table 1. The results showed that the rate of decolorization (%) of dyes depended on their chemical structure, e.g. on the nature of the

chromophore. Significant decolorization was observed by OR2 (93%) and AB (83%). In the case of other dyes, decolorization rate ranging from 53% to 68% has been achieved. Decolorization was lowest for the acridine type of dye, AO, where HRP-A removed 45% of dye. The results indicate that the acidic isoform of HRP can decolorize several types of dye.

Mass spectrometric analysis of OR2 dye before and after decolorization by HRP was carried out and the results are shown in Fig. S2. The peak at 327 *m/z* is considered as the characteristic peak of OR2 using ESI-MS in negative mode. Many peaks of different intensities and m/z were observed after dye degradation, among which some has already been reported in literature [24].

3.2. Genotoxicological assessments of dyes before and after decolorization

We measured using comet assay the DNA damaging capacity of eight dyes over a broad range of concentrations of each dye (Fig. 1). Incubation of cells with dyes (0-300 µg mL^{-1}) for 30 min increased the yield of damage in most of tested dyes. The highest level of DNA damage was induced by OR2, AO, CBB and PS and it was clearly dose dependent. There was no indication of significant DNA breakage in the case of CR, AB and RBBR.

The effect of oxidative cleavage of dye by HRP-A was further tested on OR2 and AB, as a model dyes. Three identical slides were prepared for each dye: one for measuring strand breaks (SBs), one for enzyme buffer incubation and one for incubation with FPG. From the difference in the % tail DNA between buffer incubation and FPG incubation, the net FPG-sensitive sites were obtained. OR2 causes dose-dependent strand breakage (Fig. 2A). Before decolorization, at the concentration of 300 µg mL^{-1}, cells treated with OR2 showed 23% of DNA in tail (Fig. 2A, –●–). Additional incubation with FPG led to an increase of strand breaks detected by comet assay to 53% (Fig. 2A, –▲–). Net FPG sensitive-sites after exposure to OR2 reveal that some oxidative base damage had occurred. After degradation of OR2 by HRP-A, DNA damage has decreased significantly (Fig. 2A, –▼–). No differences were seen when degradation products were incubated with FPG (Fig. 2A, –◀–).

The level of strand breaks measured after the treatment of the cells embedded in agarose with AB was low at all concentrations (Fig. 2B, –●–). The 30 min incubation with FPG does not significantly

increase damage seen (Fig. 2B, –▲–). Similar results were observed after treatment of cells with AB degradation products, once again indicating a lack of genotoxic effects (Fig. 2B, –▼–, –◄–).

3.3. DNA binding affinity of OR2 and AB before and after decolorization

The interactions of the dyes with CT-DNA have been studied by following the changes in UV-Vis absorbance spectra. The percentage of hyper/hypochromism was determined from the following equation: $[(\varepsilon_{DNA}+\varepsilon_D)-\varepsilon_B]/(\varepsilon_{DNA}+\varepsilon_D)]x100$, where ε_{DNA} is the extinction coefficient of CT-DNA, ε_D is the extinction coefficient of free dye and ε_B is the extinction coefficient of the bound dye.

The dye OR2 has two characteristic absorption bands found at 490 and 309 nm, while two smaller peaks are in the wavelength range from 251 and 261 nm (Fig. 3A, curve 2). Incubation of OR2 with CT-DNA shows no significant changes in the visible region of the spectrum, but hyperchromism of 60% was observed at 260 nm (Fig. 3A, curve 3). Incubation of hydrogen peroxide in the reaction with DNA and OR2 resulted in decrease of the absorption band at 490 and 309 nm (Fig. 3A, curve 4). The hyperchromism observed at 260 nm was much smaller than the one observed in OR2—CT-DNA spectra. Enzymatic degradation of the OR2 by HRP-A was followed by a decrease in absorption intensity at 490 and 309 nm resulting in 97% dye degradation (Fig. 3A, curve 5). A small blue shift of 3 nm was observed at 260 nm and was followed by 32% hypochromism.

The electronic absorption spectra of AB show two maxima at 620 and 320 nm, with a minor peak at ultraviolet region around 230 nm (Fig. 3B, curve 2). Incubation of the dye with CT-DNA led to a small blue shift in the 260 nm region followed by 4% hypochromism (Fig. 3B, curve 3). Similar effects were observed when the dye was incubated with CT-DNA in the presence of H_2O_2 (Fig. 3B, curve 4). Significant changes in the dye's electronic spectra were observed after enzymatic degradation by HRP-A (Fig. 3B, curve 5). The decrease in intensity of the absorption band at 620 nm was due to chromophore degradation by HRP-A. Decolorization of 94% was followed by formation of new peak at 464 nm and 332 nm (Fig.3B, curve 5). The blue shift of 6 nm in DNA absorption band is accompanied by hyperchromism, which reached the value of 8%.

With a fixed concentration of dye or degradation products, UV absorption spectra were recorded with increasing concentration of CT-DNA. The changes of the UV spectra are shown in Figure 4 and 5 for OR2 and AB, respectively. Upon the addition of increasing concentration of DNA, the intensity of the absorption band around 260 nm was increasing, but without an obvious shift in wavelength (Fig. 4A). After decolorization, the peak located at 309 nm disappeared due to dye degradation, while additions of DNA led to a small blue shift of 3 nm with flattening of the shoulder peak located around 230 nm (Fig. 4B). Addition of DNA to AB resulted in no changes in the 320 nm absorption band, while the peak at 260 nm clearly increased (Fig. 5).A small peak at 236 nm from the dye disappeared after the addition of DNA (Fig. 5A). The UV absorption band of the AB degradation products at 320 nm had significantly lower absorptivity due to dye degradation. Upon the addition of AB degradation products to DNA no spectral shifts were observed and the maximal absorption band at 320 nm did not change (Fig. 5B). Experimental results presented in this study indicate that the interactions of dyes with DNA exist, but the changes observed in the absorbance spectra of DNA and the dyes studied could not clearly indicate which mode it is.

3.4. Mode of interaction of OR2 and AB before and after decolorization

The fluorescence spectra of EB bound to DNA in the absence and presence of OR2 and degradation products of OR2 are given in Figure 6. The fluorescence intensity of the band at 596 nm decreased with increasing concentration of OR2. The maximal decrease of fluorescence intensity of EB-DNA by OR2 was 72.8%. After degradation of OR2 by HRP-A, the decrease of fluorescence intensity was significantly lower, only 33.2%. Results show that after decolorization, competitive binding of degradation products with EB is less efficient than OR2 itself.

Upon addition of OR2 the decrease in fluorescence intensity of EB—CT-DNA complex was significant (Fig. 6A). After decolorization, degradation products of OR2 have a less significant impact on the decrease of fluorescence intensity, suggesting that degradation products are less potent to quench EB from the DNA (Fig. 6B).

From the slopes of the plots (Fig. 7) the quenching constant were calculated as: K=7.62 x10^4 and 2.64 x10^4, before and after decolorization, respectively. The K values suggest that the effects of OR2 are much stronger than those after decolorization. In order to determine what type of quenching has occurred, static or dynamic, the following equation was applied : $k_q=K/\tau_0$, where k_q is the apparent biomolecular quenching rate constant and τ_0 is the fluorescence lifetime of the biomolecule in the absence of quencher, which is around 10^{-8} s^{-1} [27]. For OR2 and degraded OR2 the calculated k_q were 7.62 x10^{11} and 2.64 x10^{11} s^{-1}, respectively. Since the obtained values of k_q are greater than the maximum diffusion collision quenching rate constant of various quenchers with biopolymers, 2.0 x10^{10} M^{-1} s^{-1}, indicating that binding of OR2 and degradation products of OR2 is a static rather than dynamic collision quenching [28]. The binding constants for OR2 and degradation product were: K_B=5.33 x10^4 and 0.2 x10^4 M^{-1}, respectively.

The fluorescence spectra of EB bound to CT-DNA in the absence and presence of AB, and degradation products of AB are given in Figure 8. The fluorescence intensity of the band at 600 nm of the EB—CT-DNA decreased with the increasing concentration of AB. The maximal decrease of fluorescence intensity of EB—CT-DNA by AB was 31% (Fig. 8A) and by degradation products of AB 23% (Fig. 8B). Result show that the competition of degradation products of AB with EB in binding to DNA was less pronounced than of AB.

The quenching curve shown in Figure 8 was applied to determine K by linear regression of a plot I_0/I vs. $\boldsymbol{r}$. The corresponding quenching constant of EB—CT-DNA system by AB and degraded AB were calculated as 7.50 x 10^4 and 5.13 x10^4, respectively (Fig. 9). The apparent biomolecular quenching rate constants before and after decolorization of AB were calculated as: k_q=7.49 x 10^{11} and 5.13 x 10^{11} s^{-1}. Once again, the k_q was much greater than the limiting diffusion rate constant of the biomolecule, indicating that the binding between quencher and DNA is a static quenching process. The high linear correlation coefficient indicates that the supposed interaction was in good agreement with the first one. From the double reciprocal plot (Fig. 9B) the binding constant, K_B, for AB and degraded AB was calculated as 3.18 x10^5 and 0.65 x 10^5 M^{-1}, respectively.

4. Discussion

4.1. Decolorization study

Treatment of wastewater from several major industries presents a great challenge to today's environmental research. The textile industry is among the highest in terms of usage of fresh water and generation of colored wastewaters. The great varieties of synthetic dyes used present a challenge for biodegradation studies, because of the diverse structure of dyestuffs. Over the past decades plant peroxidase, especially HRP, has been applied successfully in decolorization of various types of dyes. Although there are numerous reports about the relation between the degradability and molecular structure of dyes, the general outcome is still unclear [29]. Some reports indicated that the decolorization of single azo dyes is easily than of the double azo [2]. The present investigation and earlier observations are in agreement with this [22]. Nevertheless, the ultimate aim of bioremediation should be the reduction of toxicity, not only the concentration of the environmental pollutant.

4.2. Genotoxicity study

Various methods for treatment of colored wastewater have been developed so far, but the toxicity analysis of its metabolites or degradation products is to be one of the prime responsibilities in the view of environmental remediation [30]. The parent dye molecules differ in chemical and biological properties from the hydrolyzed form which is the one found in the effluent [31]. An obvious indicator of dye removal is the loss of color, but the presence of the products or metabolites can create problems [32]. The possibility of producing a genotoxic and carcinogenic amine during degradation process is high [10]. Besides, azo derived dyes can generate NO_2 and ROS which are able to damage DNA and other cellular structures [33]. Thus, the carcinogenic effects of azo dyes could be derived from the direct action of dyes on the cells. Damage to cell DNA following interaction with toxic compound causes mutations [11,34]. The use of toxicity bioassays is extremely important to evaluate not only the effectiveness of a treatment but also the degree of its environmental safety [35]. The comet assay has a great advantage since it gives a response at the level of DNA and if applied as an *in vitro* test is more specific than other genotoxicity methods [25]. In the literature anthraquinone dyes have been reported

to induce mutagenicity, but there was a negative response in the alkaline comet assay with NDHF cell [18]. In our case, RBBR (anthraquinone dye) showed a slight increase of DNA damage with increase of dye concentration. Most DNA damage was induced by CBB, a triphenylmethane dye (Fig. 1). Double azo, reactive dye, Red HE3B was found to induce high DNA damage on the nuclei from the root meristem cells of *A. cepa* bulbs most probably via oxidative stress during dye exposure [36]. Some reports indicate that the genotoxic effects observed with the comet assay after HepG2 cells were exposed to two azo dye (Basic Red 51 and Basic Brown 19) were due to their azo structure [33]. In our case, the tested double azo dyes (CR, AB, PS and RB5) exhibit different percentage of DNA breaks in the BEAS-2B cells. When the DNA is incubated with FPG, after the lysis of cells embedded in agarose, extra breaks are seen. FPG acts primarily at 8-oxo-7,8-dihydroguanine (8-oxoGua), which is a product of DNA oxidation by ROS. The frequency of net FPG-sensitive sites, gives the reflection of altered bases in DNA [37]. We have applied a bacterial lesion-specific endonuclease to increase the number of DNA breaks present, in order to make a comet assay more sensitive. In the present studies OR2 (single azo dye) showed an increase in FPG-sensitive sites, by modified comet assay, revealing oxidized bases after 30 incubation, which was not the case for OR2 degradation products (Fig. 2A). Significant toxic effects on the white rod fungus *S.commune* was reported by Renganathan, which is caused by increase in lag phase due to bioaccumulation of OR2 [38]. Azoreductase enzymes can metabolize dyes producing free aromatic amines that are potentially carcinogenic and mutagenic [34]. In the case of AB (double azo dye) in spite of increasing dye or dye degradation products concentration there was no increase in SB or FPG-sensitive sites (Fig. 2B).

4.3. DNA interaction study

UV-Vis spectroscopy is a useful method to investigate the binding modes of dyes with CT-DNA. Binding to the CT-DNA can be at different positions and by formation of different bonds, such as covalent of non-covalent. In non-covalent mode of DNA interaction the molecules can bind by intercalation, like groove binders or by electrostatic interactions [39]. The hyperchromism and hypochromism are regarded as spectral evidence for the changes in DNA double-helix structure [40]. Contraction of CT-DNA in the helix axis usually results in hypochromism, followed by changes in the

conformation as well [41]. This is shown in the UV-visible absorption spectrum of OR2 (Fig. 3A), where the hypochromism at 260 nm was followed with small blue shift. This could indicate possibly damaging of the CT-DNA double-helix structure by the dye. Degradation products of OR2 after enzymatic decolorization by HRP was proposed by Zhang, indicating three possible way of degradation: asymmetrical splitting of C-N bond, symmetrical cleavage of the azo bond and coupling reaction between by-products and parent dye molecule. Using ESI-TOF-MS analysis four degradation products detected were proposed to be: 1,2-dihydroxynaphtalene, 4-hydroxybenzenesulfonate, 4-nitrosobenzenesulfonate and complex polymers of 1,2-dihydroxynaphtalene and dye [24]. This significantly differs from toxic moieties identified after microbial degradation of OR2 such as: 1-amino-2-naphtol and 4-amino-benzenesulfonic acid [31,42]. Similarly, when AB was subjected to photo catalytic degradation by UV/H_2O_2 three possible pathway of degradation was observed leading to formation of 11 degradation products which was highly dependent upon reaction conditions [43]. Considering above stated, the reduction in reactivity of degradation products in case of OR2 could be explained by the lack of aromatic amine after HRP treatment.

4.4. Competitive binding studies with ethidium bromide

Ethidium bromide is a very sensitive fluorescent probe which binds to DNA with strong affinity *via* intercalation. The extent of fluorescence quenching of EB from EB—CT-DNA complex is a measure of the strength of interaction between the second molecule and DNA. The changes in fluorescent spectra resulting from titration of a preformed EB—CT-DNA complex with dye and degradation products were measured (Fig. 6 and 8). These effects were much more pronounced with dye before, than after degradation. Such occurrence could be result of competition for EB binding sites on DNA (1), dye and fluorescent probe molecules form a compound which reduces the EB binding to DNA (2), formation of a new non-fluorescent complex between the dye, EB and CT-DNA (3). Since there were no changes in the fluorescent intensity of dye or degradation products after the addition of EB (data not shown) the second phenomenon is less likely. The addition of dye to EB—CT-DNA caused a decrease of fluorescence intensity at the very beginning of titration, leading to the conclusion that quenching was a result of a competition of dye for an EB binding sites on the DNA. This effect was

more pronounced in case of OR2 than AB. The experimental results indicate that the quenching process in both cases were static quenching. The K_B value for degradation products suggests that the effects of dyes are stronger than those of HRP-A decolorization products. The results showed that the dyes inhibit binding of the intercalator, EB, indicating possible degradation of DNA, which was less extensive with degradation products.

5. Conclusions

The ascertaining of DNA damage is of great importance since the significance as a cancer precursor is clear. Our findings suggest that by enzymatic degradation of Orange II with HRP-A DNA damage was decreased. Also, the degradation products had no DNA damaging effects in BEAS-2B cells. While the comet assay is powerful technique certain limitation must be taken into account with the cell system applied. Although, BEAS-2B cell line has a wide application in the biological endpoint assessment, it is important to highlight that some metabolism capabilities limitation in this cell line do exist. Enzymatic degradation is known to break the azo bonds in the dye molecule which can sometimes lead to accumulation of aromatic compounds with higher reactivity than the parent dye molecule. For that reason, AB as a di azo dye, has been taken as a model dye to investigate the effects of enzymatic degradation with HRP. The ecogenotoxicological potential of this enzymatic method for dye decolorization was confirmed in terms of elimination of the genotoxicity potential of the dye tested. The comet assay can be easily and successfully employed for assessment of DNA damage by dyes and degradation products and should be applied in the future to monitor waste water treatment. The more detailed DNA interaction studies on CT-DNA supported these results. Structural differences of the OR2 and AB most definitely play a role in different competitive binding. The detailed identification and analysis of dye degradation product would greatly help in bridging the gap between dye structure and toxicity but the question of environmental conditions in which the reaction will take place still remain.

Acknowledgements

This work was supported by the Ministry of Education, Science and Technological Development of Republic of Serbia (Grant 172048). B.J. was supported by the FEBS Collaborative Experimental Scholarship during her research stay in Oslo, Norway.

References

[1] S. Husain, F. Jafri, M. Saleemuddin, Immobilization and stabilization of horseradish peroxidase isoforms, Biochem. Mol. Biol. Int. 40 (1996) 1–11.

[2] A.U. Chaudhari, S.R. Tapase, V.L. Markad, K.M. Kodam, Simultaneous decolorization of reactive Orange M2R dye and reduction of chromate by Lysinibacillus sp. KMK-A, J. Hazard. Mater. 262 (2013) 580–588. doi:10.1016/j.jhazmat.2013.09.006.

[3] E. Forgacs, T. Cserhti, G. Oros, Removal of synthetic dyes from wastewaters: A review, Environ. Int. 30 (2004) 953–971. doi:10.1016/j.envint.2004.02.001.

[4] F. Jamal, Functional Suitability of Soluble Peroxidases from Easily Available Plant Sources in Decolorization of Synthetic Dyes, (2006).

[5] N. Lončar, B. Janović, M. Vujčić, Z. Vujčić, Decolorization of textile dyes and effluents using potato (Solanum tuberosum) phenoloxidase, Int. Biodeterior. Biodegrad. 72 (2012) 42–45. doi:10.1016/j.ibiod.2012.05.001.

[6] F.W. Krainer, A. Glieder, An updated view on horseradish peroxidases: recombinant production and biotechnological applications, Appl. Microbiol. Biotechnol. 99 (2015) 1611–1625. doi:10.1007/s00253-014-6346-7.

[7] Q. Husain, Peroxidase mediated decolorization and remediation of wastewater containing industrial dyes: A review, Rev. Environ. Sci. Biotechnol. 9 (2010) 117–140. doi:10.1007/s11157-009-9184-9.

[8] A. Bhunia, S. Durani, P.P. Wangikar, Horseradish Peroxidase Catalyzed Important Dyes, Biotechnol. Bioeng. 5 (2001) 562–567.

[9] C. Regalado, B.E. García-Almendárez, M. a. Duarte-Vázquez, Biotechnological applications of peroxidases, Phytochem. Rev. 3 (2004) 243–256.

[10] K. Schneider, C. Hafner, I. Jäger, Mutagenicity of textile dye products, J. Appl. Toxicol. 24

(2004) 83–91. doi:10.1002/jat.953.

[11] H. Ben Mansour, D. Barillier, D. Corroler, K. Ghedira, L. Chekir-Ghedira, R. Mosrati, In vitro study of DNA damage induced by acid orange 52 and its biodegradation derivatives., Environ. Toxicol. Chem. 28 (2009) 489–495. doi:10.1897/08-333.1.

[12] F. Maria, D. Chequer, D.J. Dorta, D.P. De Oliveira, Azo Dyes and Their Metabolites : Does the Discharge of the Azo Dye into Water Bodies Represent Human and Ecological Risks ?, Adv. Treat. Text. Effl. (2011) 27–48. doi:10.5772/19872.

[13] A. Mittal, V. Thakur, V. Gajbe, Adsorptive removal of toxic azo dye Amido Black 10B by hen feather, (2013) 260–269. doi:10.1007/s11356-012-0843-y.

[14] A. Garg, M. Mainrai, S. Barman, Experimental Investigation on Adsorption of Amido Black 10B Dye onto Zeolite Synthesized from Fly Ash, Chem. Eng. Commun. 6445 (2015). doi:10.1080/00986445.2013.836636.

[15] T. Gan, J. Sun, Z. Lin, Y. Li, Highly sensitive determination of Orange II based on the dual amplified electrochemical signal of graphene, Anal. Methods. 5 (2013) 2964–2970. doi:10.1039/c3ay40250a.

[16] SCCS (Scientific Committee on Consumer Safety), Opinion on Acid Orange 7, 22 March 2011, 2011. doi:10.2772/96785.

[17] A. Yadav, A. Kumar, P. Dhar, A. Tripathi, M. Das, In vitro studies on immunotoxic potential of Orange II in splenocytes, Toxicol. Lett. 208 (2012) 239–245. doi:10.1016/j.toxlet.2011.11.014.

[18] D.M. Leme, G.A.R. de Oliveira, G. Meireles, T.C. dos Santos, M.V.B. Zanoni, D.P. de Oliveira, Genotoxicological assessment of two reactive dyes extracted from cotton fibres using artificial sweat, Toxicol. Vitr. 28 (2014) 31–38. doi:10.1016/j.tiv.2013.06.005.

[19] A.R. Collins, Measuring oxidative damage to DNA and its repair with the comet assay, BBA -

Gen. Subj. 1840 (2014) 794–800. doi:10.1016/j.bbagen.2013.04.022.

[20] A. Azqueta, S. Shaposhnikov, A.R. Collins, DNA oxidation : Investigating its key role in environmental mutagenesis with the comet assay, Mutat. Res. 674 (2009) 101–108. doi:10.1016/j.mrgentox.2008.10.013.

[21] C. Garcia-Canton, E. Minet, A. Anadon, C. Meredith, Metabolic characterization of cell systems used in in vitro toxicology testing: Lung cell system BEAS-2B as a working example, Toxicol. Vitr. 27 (2013) 1719–1727. doi:10.1016/j.tiv.2013.05.001.

[22] Z. Vujcic, B. Janovic, N. Loncar, A. Margetic, N. Bozic, B. Dojnov, et al., Exploitation of neglected horseradish peroxidase izoenzymes for dye decolorization, Int. Biodeterior. Biodegradation. 97 (2014) 124–127. doi:10.1016/j.biod.2014.10.007.

[23] M. Estela da Silva, T.T. Franco, Purification of soybean peroxidase (Glycine max) by metal affinity partitioning in aqueous two-phase systems, 743 (2000) 287–294.

[24] A. Zhang, L. Fang, J. Wang, W. Liu, Enzymatic Decolorization of Orange II: Optimization by Response Surface Methodology and Pathway, Environ. Prog. Sustain. Energy. 32 (2013) 294–301. doi:DOI 10.1002/ep.

[25] A. Azqueta, A.R. Collins, The essential comet assay: A comprehensive guide to measuring DNA damage and repair, Arch. Toxicol. 87 (2013) 949–968. doi:10.1007/s00204-013-1070-0.

[26] M.T. Vujčić, S. Tufegdžić, I. Novaković, D. Djikanović, M.J. Gašić, D. Sladić, Studies on the interactions of bioactive quinone avarone and its methylamino derivatives with calf thymus DNA, Int. J. Biol. Macromol. 62 (2013) 405–410. doi:10.1016/j.ijbiomac.2013.09.013.

[27] Y. Shi, C. Guo, Y. Sun, Z. Liu, F. Xu, Y. Zhang, et al., Interaction between DNA and Microcystin-LR Studied by Spectra Analysis and Atomic Force Microscopy, (2011) 797–803.

[28] S. Bi, C. Qiao, D. Song, Study of interactions of flavonoids with DNA using acridine orange as a fluorescence probe, 119 (2006) 199–208. doi:10.1016/j.snb.2005.12.014.

[29] T.S. Shaffiqu, J. Roy, R.A. Nair, T.E. Abraham, Degradation of Textile Dyes Mediated by Plant Peroxidases, Appl. Biochem. Biotechnol. 102-103 (2002) 315–326.

[30] S.S. Phugare, D.C. Kalyani, S.N. Surwase, J.P. Jadhav, Ecofriendly degradation, decolorization and detoxification of textile effluent by a developed bacterial consortium, Ecotoxicol. Environ. Saf. 74 (2011) 1288–1296. doi:10.1016/j.ecoenv.2011.03.003.

[31] A. Gottlieb, C. Shaw, A. Smith, A. Wheatley, S. Forsythe, The toxicity of textile reactive azo dyes after hydrolysis and decolourisation, J. Biotechnol. 101 (2003) 49–56. doi:10.1016/S0168-1656(02)00302-4.

[32] R. V. Khandare, S.P. Govindwar, Phytoremediation of textile dyes and effluents: Current scenario and future prospects, Biotechnol. Adv. 33 (2015) 1697–1714. doi:10.1016/j.biotechadv.2015.09.003.

[33] Y. Tafurt-Cardona, P. Suares-Rocha, T.C.C. Fernandes, M.A. Marin-Morales, Cytotoxic and genotoxic effects of two hair dyes used in the formulation of black color, Food Chem. Toxicol. 86 (2015) 9–15. doi:10.1016/j.fct.2015.09.010.

[34] C. V. Uliana, G.S. Garbellini, H. Yamanaka, Spectrophotometric evaluation of the behavior of disperse red 1 dye in aqueous media and its interaction with calf thymus ds-DNA, J. Braz. Chem. Soc. 23 (2012) 1469–1475. doi:10.1590/S0103-50532012005000009.

[35] M.C. Silva, J.A. Torres, L.R. Vasconcelos De Sá, P.M.B. Chagas, V.S. Ferreira-Leitão, A.D. Corrêa, The use of soybean peroxidase in the decolourization of Remazol Brilliant Blue R and toxicological evaluation of its degradation products, J. Mol. Catal. B Enzym. 89 (2013) 122–129. doi:10.1016/j.molcatb.2013.01.004.

[36] S.S. Phugare, D.C. Kalyani, A. V. Patil, J.P. Jadhav, Textile dye degradation by bacterial consortium and subsequent toxicological analysis of dye and dye metabolites using cytotoxicity, genotoxicity and oxidative stress studies, J. Hazard. Mater. 186 (2011) 713–723. doi:10.1016/j.jhazmat.2010.11.049.

[37] A. Azqueta, L. Arbillaga, A. L??pez De Cerain, A. Collins, Enhancing the sensitivity of the comet assay as a genotoxicity test, by combining it with bacterial repair enzyme FPG, Mutagenesis. 28 (2013) 271–277. doi:10.1093/mutage/get002.

[38] S. Renganathan, W.R. Thilagaraj, L.R. Miranda, P. Gautam, M. Velan, Accumulation of Acid Orange 7, Acid Red 18 and Reactive Black 5 by growing Schizophyllum commune, Bioresour. Technol. 97 (2006) 2189–2193. doi:10.1016/j.biortech.2005.09.018.

[39] K.R. Sangeetha Gowda, B.B. Mathew, C.N. Sudhamani, H.S.B. Naik, Mechanism of DNA Binding and Cleavage, Biomed. Biotechnol. 2 (2014) 1–9. doi:10.12691/bb-2-1-1.

[40] N. Shahabadi, M. Maghsudi, Gel electrophoresis and DNA interaction studies of the food colorant quinoline yellow, Dye. Pigment. 96 (2013) 377–382. doi:10.1016/j.dyepig.2012.09.004.

[41] C. Tong, Z. Hu, J. Wu, Interaction between methylene blue and calfthymus deoxyribonucleic acid by spectroscopic technologies, J. Fluoresc. 20 (2010) 261–267. doi:10.1007/s10895-009-0549-9.

[42] D. Rawat, V. Mishra, R.S. Sharma, Chemosphere Detoxification of azo dyes in the context of environmental processes, Chemosphere. 155 (2016) 591–605. doi:10.1016/j.chemosphere.2016.04.068.

[43] M.A. Meetani, S.M. Hisaindee, F. Abdullah, S.S. Ashraf, M.A. Rauf, Chemosphere Liquid chromatography tandem mass spectrometry analysis of photodegradation of a diazo compound : A mechanistic study, Chemosphere. 80 (2010) 422–427. doi:10.1016/j.chemosphere.2010.04.065.

Fig. 1. Assessment of genotoxic effects in BEAS-2B cells exposed to different concentration of dyes (3, 10, 30, 100 and 300 μg mL^{-1}) and negative control (PBS) measured by the comet assay. DNA damage was presented as mean value of DNA breaks measured through DNA tail parameter (y-axis) at each dye concentration (bar). The experiments were conducted in triplicate and repeated three times. The

significant difference between dye, concentration and the control (PBS) was confirmed by Two-way ANOVA at $P < 0.05$.

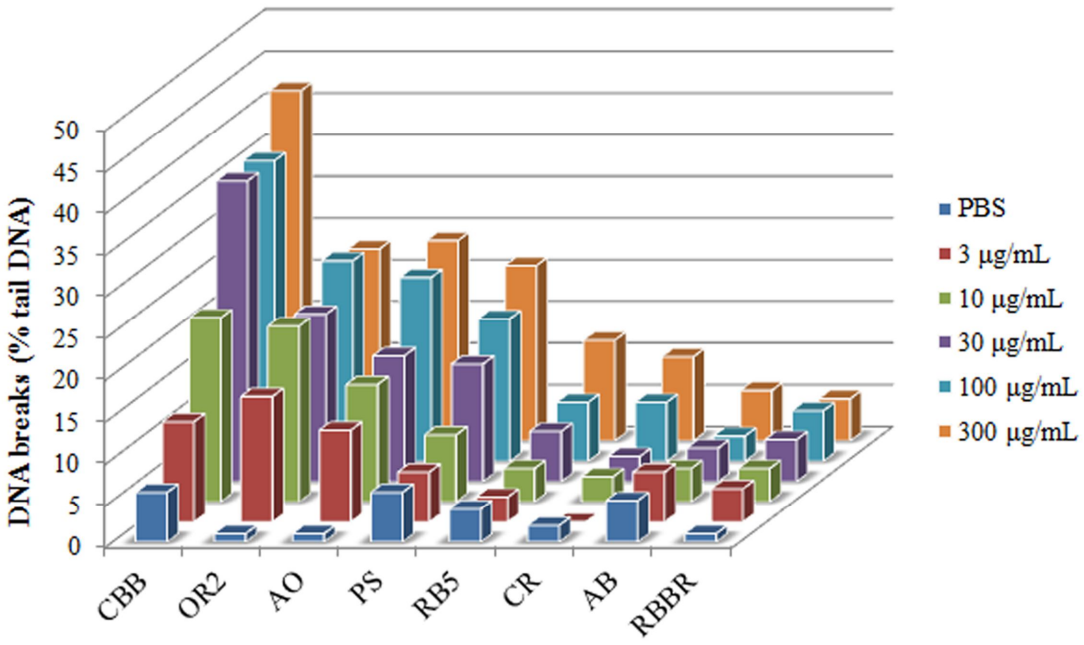

Fig. 2. DNA oxidation damage in BEAS-2B cells exposed to dye and degradation products using comet assay, FPG sensitive sites. A) OR2, B) AB. Values are means of three experiments, ±SD, significantly different from the control (PBS) at, *$P < 0.05$, *** $P < 0.01$, by One-way ANOVA with Tukey-Kramer comparison test.

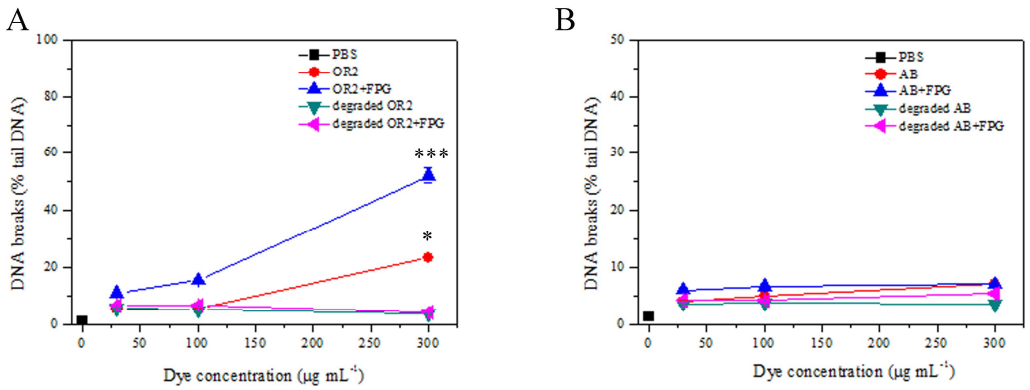

Fig. 3. The changes in the absorption spectra of OR2 (A, 30 µg L^{-1}) and AB (B, 30 µg L^{-1}) before and after decolorization by HRP-A (0.14 U mL^{-1}) in the presence of H_2O_2 (6.25 µg mL^{-1}). Curve 1 – CT-DNA (9 x 10^{-5} mol L^{-1}); curve 2 – dye, curve 3 – dye—CT-DNA complex; curve 4 – dye—CT-DNA complex with H_2O_2 ; curve 5 – dye degradation product with CT-DNA.

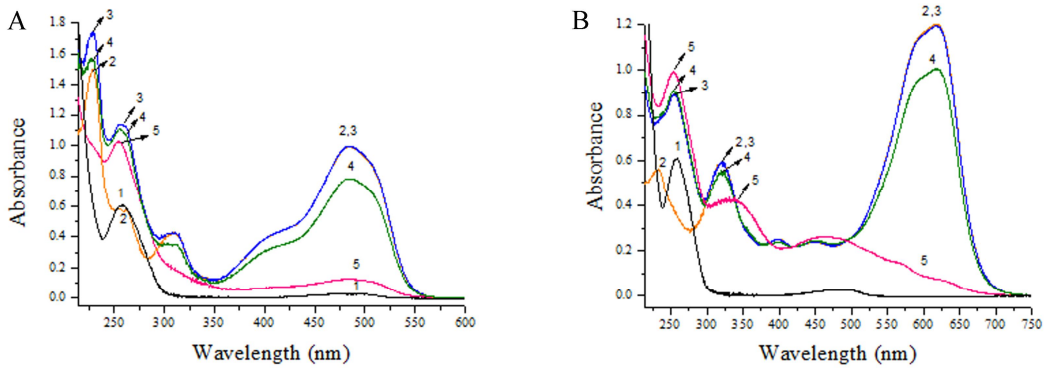

Fig. 4. Interaction of 35 µM OR2 before (A) and after (B) decolorization in the presence of 0, 23, 46, 92, 115, 138, 162, 185 and 208 µM CT-DNA (the arrow indicates the direction of changes).

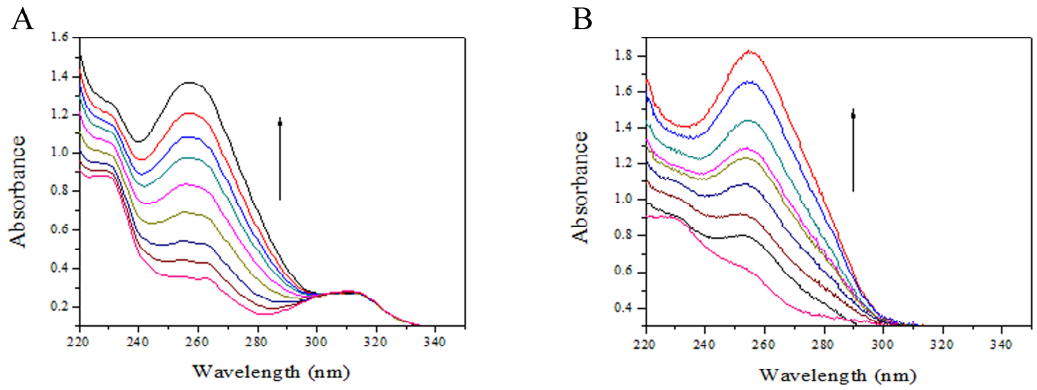

Fig. 5. Interaction of 33 µM AB before (A) and after (B) decolorization in the presence of 0, 23, 46, 92, 115, 138, 162, 185 and 208 µM CT-DNA (the arrow indicates the direction of changes).

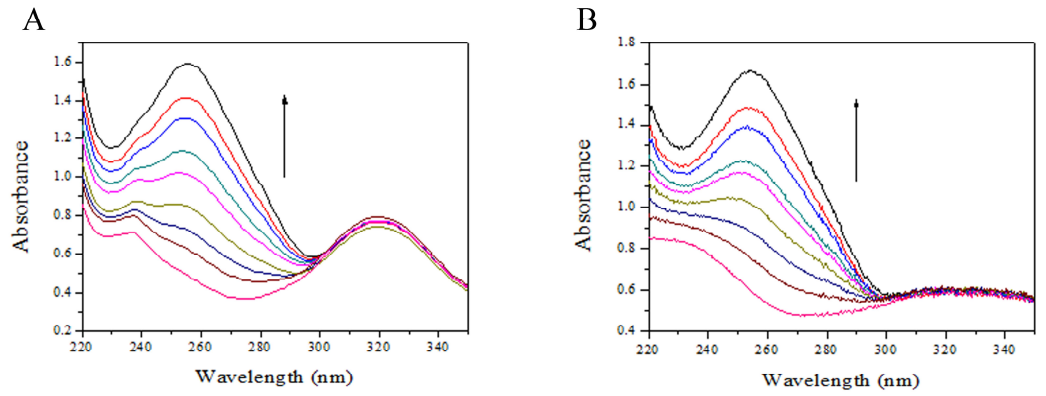

Fig. 6. Fluorescence spectra of EB—CT-DNA system in the presence of OR2 (A) and its degradation products (B) at various concentrations of dye or decolorization products (0, 2.7, 5.7, 8.2, 10.7, 12.9 and 15.2 μM). Concentrations of EB and CT-DNA were 25μM and 100μM, respectively. The arrows indicates the direction of changes.

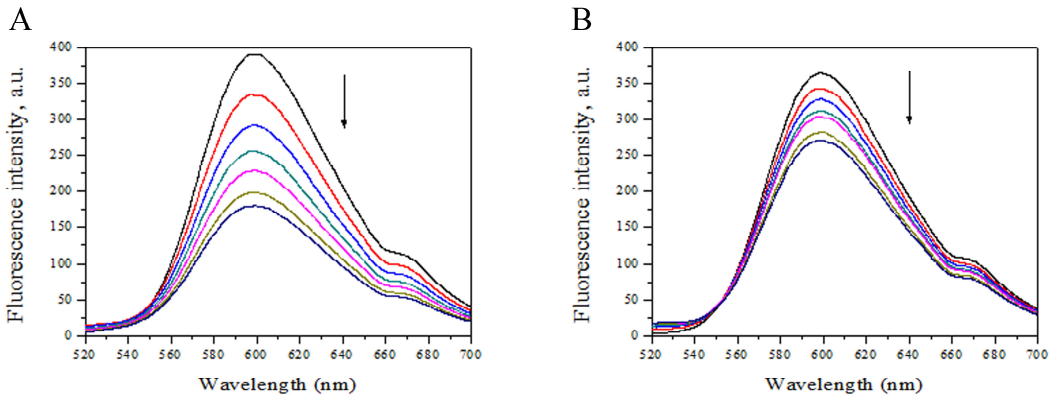

Fig. 7. Modified Stern-Volmer plot of fluorescence quenching curves of EB—CT-DNA system (A) by OR2 (before decolorization) and degradation products (after decolorization) at λ_{max}=600nm; (B) Double reciprocal plot of 1/(F_0-F) vs.1/ [Q] for adding various amount of OR2 to the EB—CT-DNA before (■) and after decolorization (●). F_0 and F present the fluorescence intensity of EB—CT-DNA after the addition of dye or degradation products of OR2.

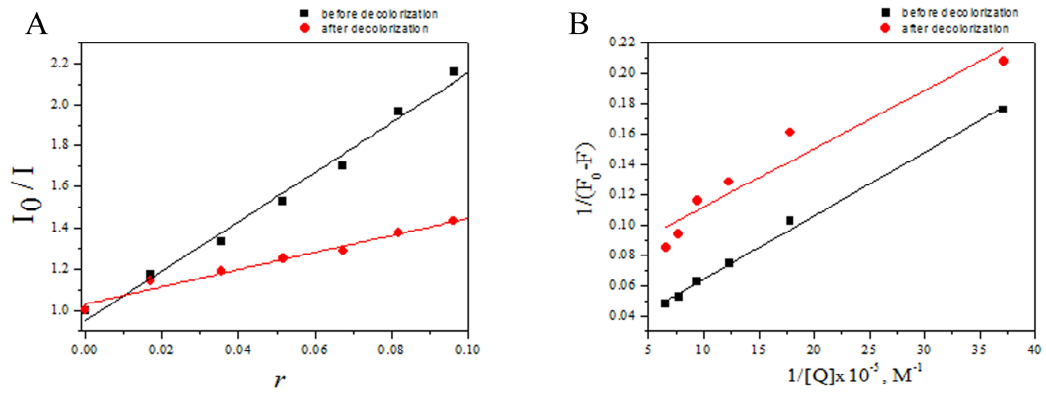

Fig. 8. Fluorescence spectra of EB—CT-DNA system in the presence of AB (A) and degradation products (B) at various concentrations of dye or decolorization products at concentration of 0, 1, 2, 3, 4, 5 and 6 μM. The concentrations of EB and CT-DNA were 25μM and 100μM, respectively. The arrows indicate the direction of changes.

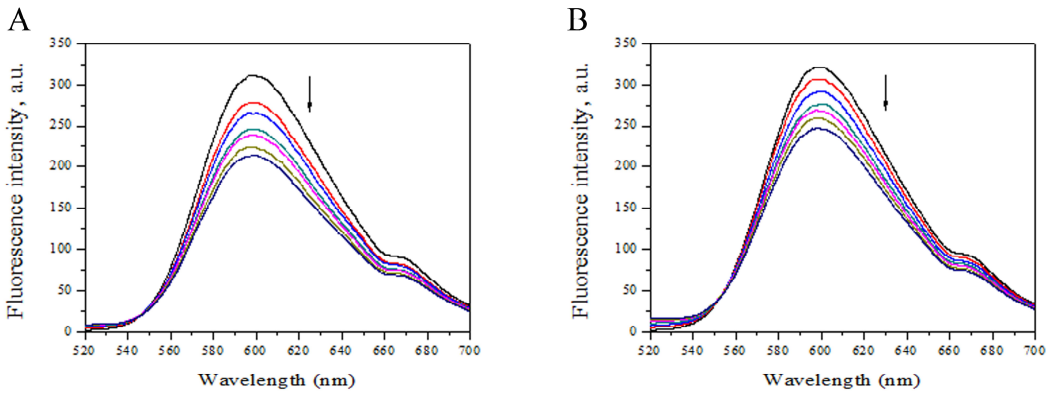

Fig. 9. Modified Stern-Volmer plot of fluorescence quenching curves of EB—CT-DNA system (A) by AB (■) and degradation products of AB (●) at λ_{max}=600nm; (B) Double reciprocal plot of $1/(F_0-F)$ vs.$1/[Q]$ for adding various amount of AB before (■) and after decolorization (●) to the EB—CT-DNA. F_0 and F present the fluorescence intensity of EB—CT-DNA after the addition of dye or degradation products of AB.

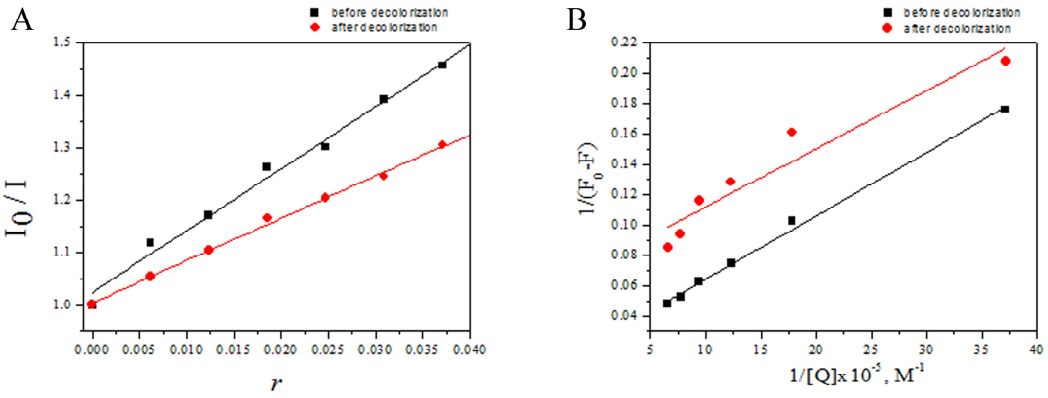

Table 1. Decolorization study of dyes by HRP-A.

Dye (Abbreviation)	C.I. Name*	Class (by the nature of the chromophore)	Decolorization** (%)
Orange II (OR2)	Acid Orange 7	Single azo	93.51 ± 5.07
Amido Black 10B (AB)	Acid Black 1	Double azo	83.25 ± 4.58
Ponceau S (PS)	Acid Red 112	Double azo	56.73 ± 3.40
Congo Red (CR)	Direct Red 28	Double azo	53.67 ± 9.07
Acridine Orange (AO)	Solvent Orange 15	Acridines	45.63 ± 11.53
Coomassie Brilliant Blue (CBB)	Acid Blue 83	Triphenylmethane	76.03 ± 8.54
Cibacron Navy DP-B (RB5)	Reactive Black 5	Double azo	68.51 ± 1.51
Remazol Brilliant Blue R (RBBR)	Reactive Blue 19	Anthraquinone	71.67 ± 3.05

*C.I.Name: Colour Index (International) Name. ** Data presented as mean ± standard deviation.